

# Development of Surrogate Hand for Impact Tests

Trevor A. Brison, Eduardo M. Sosa

West Virginia University Department of Mechanical and Aerospace Engineering

Despite continuous advancements in technology and safety procedures, hand injuries are still a significant problem in many industries. Metacarpal gloves are often used by workers to protect their hands against impacts, cuts, and other hazards. Importantly, testing the level of impact protection offered by different designs of metacarpal gloves cannot be done with living subjects. This limitation requires the use of a surrogate hand which can be used consistently and systematically in controlled impact tests. This work focuses on the development of a surrogate hand which can be manufactured and used for this purpose. The surrogate hand developed in this work is comprised of a bone structure and a flexible synthetic gel material, and the hand design is based on digital models obtained through laser scanning of bone and hand shapes. These digital models were scaled and assembled using a mesh editing software to generate a representative hand with the required size and posture. The resulting hand model was materialized with a 3D-printed bone structure surrounded by synthetic gel with shape, proportions, and flexibility resembling that of an actual hand.

## Introduction

Hand injuries are a significant and common ailment in many industries, and even with advancements in technology and safety procedures, physical tasks which can produce hand injuries still exist<sup>1</sup>. For example, in the mining industry from 2000 to 2018, there were nearly 42,000 reported accidents involving the hands of miners. This number of incidents represents almost 20% of the total number of reported accidents. 76% of these accidents typically involved the fingers and thumb, while the remaining 24% involve other portions of the hand (not including the wrist)<sup>2,3</sup>. The most common preventive measure against such hand injuries are protective gloves—namely, metacarpal gloves—which are commonly used in different manufacturing and extractive industries. These gloves are designed to protect hands against lacerations and impacts, among other workplace hazards. At the time of this study, there were at least forty-five glove manufacturers operating in North America which produced a variety of industrial gloves<sup>4</sup>.

Metacarpal gloves are usually comprised of a set of fabric layers with external reinforcements made of thermoplastic rubber

(TPR), which are intended to provide impact protection. The TPR reinforcements are generally placed in segments located on top of the fingers, knuckles, and thumb, or the dorsal metacarpal region of the hand. Other models include thick pads placed over the top and bottom surfaces of the glove. Despite the variety of metacarpal glove designs and providers, one aspect of the protection which is vaguely or sparsely referenced is the performance of metacarpal gloves against an impact hazard<sup>5</sup>.

Due to a lack of consistent evaluations, there is uncertainty concerning the protective qualities of existing metacarpal gloves. Considering that it is not possible to use live hands to assess the impact protection of metacarpal gloves, an anatomically accurate and mechanically similar surrogate hand is needed to further evaluate the dampening qualities of metacarpal gloves. We previously created such a surrogate hand and successfully used it for preliminary impact testing of selected metacarpal gloves<sup>6</sup>. Here, we detail the methodology to create the surrogate hand used for those tests. The main objective of this methodology is to define a series of steps to create an anatomically accurate surrogate hand

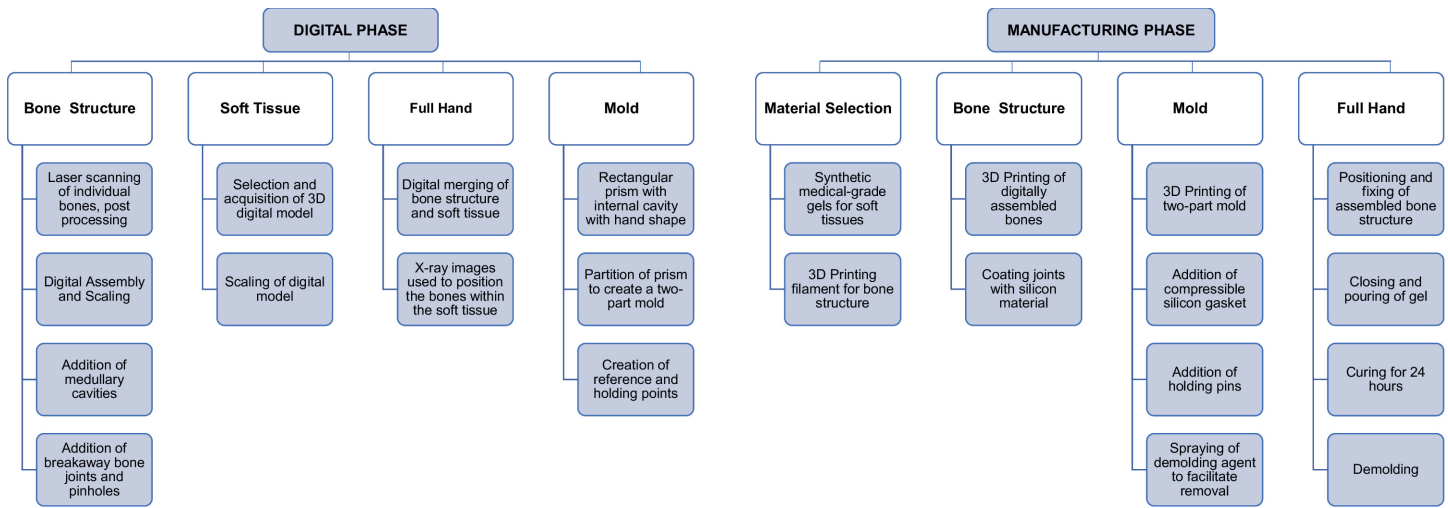


**Figure 1. Components of digital and manufacturing phases.**

which can be manufactured consistently and used for further evaluation of the impact resistance of metacarpal gloves. Achieving this objective required the development of a series of steps to create the different parts which comprise the surrogate hand. In addition, measures of the performance of the surrogate hands manufactured following the proposed methodology are included.

## Methods

The surrogate hand developed in this work consists of two main components: the bone structure (comprised of phalanges, metacarpal and carpal bones) and a soft material representative of the soft hand tissues (without a specific distinction between skin, fat, muscles, tendons and ligaments). The development of the surrogate hand was completed in two main phases: a digital phase and a manufacturing phase (Figure 1).

### Digital Phase – Bone Structure

The hand bone structure was created by laser-scanning the 27 bones of the human hand, which were provided by the WVU School of Medicine, Department of Pathology, Anatomy, and Laboratory Medicine (Figure 2A). A digital version of each bone was obtained using a laser scanner (NextEngine, Santa Monica, CA). The scanning process required

fixing bones on a rotary platform in order for the laser scanner (Figure 2B) to capture multiple still images of the bones needed to create a three-dimensional digital model (“mesh”) of each bone (Figure 2C). These images were assembled following reference points marked on the bones.

After the 27 bone meshes were created, they were imported into CAD/CAM software (Fusion360, Autodesk, San Rafael, CA) for post-processing and assembly. The post-processing involved repairs for closing the mesh body and for smoothing the surfaces to eliminate gaps and inconsistencies. The repairs ensured that all nodes of the mesh were connected correctly and formed a “watertight” bone file. The individual bones were then assembled to generate a digital version of a hand in a relaxed, opened palm position. The entire bone assembly (Figure 2E) was scaled to fit the dimension of an average-sized human hand. Measurements on X-rays (Figure 2D) and existing skeletal hand models were used to validate the anatomical accuracy of the digital assembly. The carpal region of the bone assembly was then fused to the contact region except for the trapezium carpal bone to allow subsequent articulation of the thumb. The post-processing also included the addition of medullary cavities to the metacarpals and phalanges. The dimensions of these cavities was determined based on previous observations<sup>7,8</sup> (Figure 2D). Additional minor

additions were implemented to simplify the fabrication process by creating a streamlined radius and ulna, breakaway bone joints, and pinholes to fix the bones in a mold.

### Digital Phase – Soft Tissue

The creation of a hand model compatible with the developed bone structure involved selecting and acquiring a commercially-available digital hand model with accurate anatomical features in a relatively flat position and suitable for subsequent fabrication of testing prototypes. A hand model created by Ubersculpts (CGTrader 3D Modeling, New York,

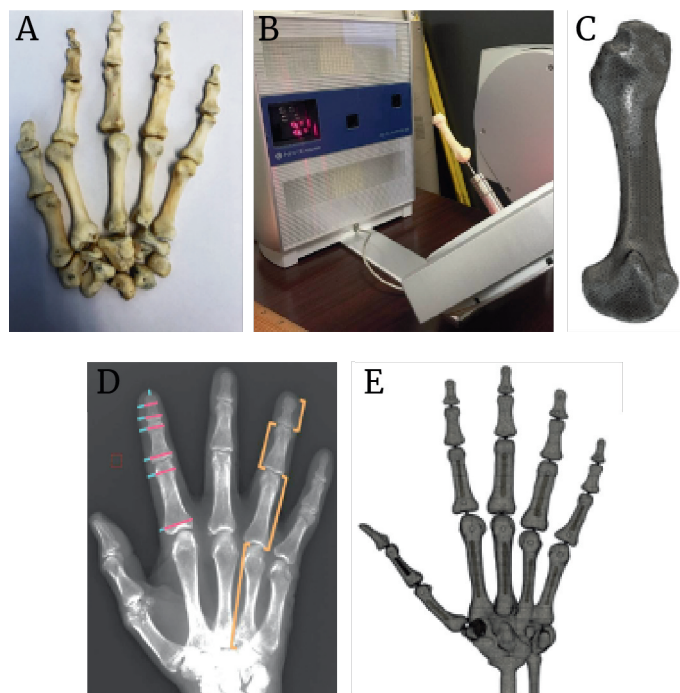


**Figure 2. Bone structure, proportions, and dimensions.** (A) left-hand bones, (B) laser scanning of individual bones, (C) digital version of middle digit metacarpal bone #3, (D) measurements from radiographic images, (E) digitally scaled and reassembled bone structure

NY) was selected due to its high mesh density, anatomical accuracy, multiple hand orientation options, and scalability (Figure 3A-C). This model needed minor modifications to fit the bone assembly and small adjustments to fit average human hand dimensions<sup>9-11</sup>. The flat hand position was selected to match the

configuration of the experimental setup used for preliminary impact tests reported previously<sup>6</sup>. The final step for the creation of the digital hand consisted of merging the bone assembly with the soft tissue portion to create the full digital hand model. The position of the bones in the resulting hand was re-verified against X-ray images of actual hands to ensure proper fitting within the hand volume.

### Digital Phase – Hand Mold

The mold for manufacturing the surrogate hands was developed based on the requirements of being scalable and 3D-printable. To construct the mold, Fusion360 software was used to generate a rectangular prism and a negative cavity within the prism. This prism was divided into two parts by a reference plane which split the mold body into two separate parts. The position of the reference plane was carefully selected to allow for easy cast removal from the mold without distorting the organic shape of the hand. Each of the mold halves included leader pins and slots to guide and join the halves when pouring the cast materials. The mold halves also included smaller pins to support and maintain the bone structure during casting (Figure 3D-F). The locations of the pins alternated between the top and bottom of each articulate bone section to prevent any movement during the casting process. The pouring sequence was designed to minimize the formation of air pockets within the cavity, such that any bubbles formed during casting could be removed with light percussive assistance. The product was a two-part mold which can hold the bone structure in place while casting molten gel material (Figure 3F).

### Manufacturing Phase – Material Selection

The digital models described previously were materialized by a combination of 3D printing of the bone structure and casting of medical-grade synthetic gel for the soft tissues in a 3D-printed two-part mold derived from the digital hand models. The decision to use

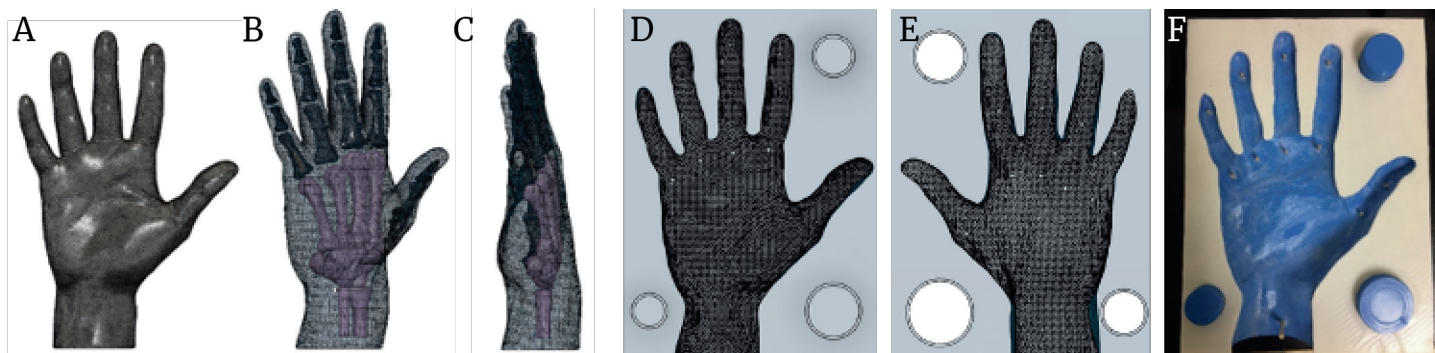


**Figure 3. Digital hand and mold models.** (A) external shape, (B) bone cavities dorsal view, (C) lateral view, (D) digital top half of mold, (E) digital bottom half of mold, (F) 3D-printed bottom half of mold

medical-grade synthetic gel to represent the soft tissues of the hand drove the selection of 3D printing materials for the bone assembly and the mold. Two grades of synthetic gel were used for this work: gels #0 and #4, (Humimic Medical, Greenville, SC). The melting temperatures of these two gel types ranged from 116°C to 121°C, which constrained the selection of 3D printing materials for the bone assembly and mold.

The chief requirement of the 3D printing material for the bone assembly was a strength and density similar to that of human bones<sup>13</sup>. Additionally, the melting temperature of the bone material must have been higher than the melting temperature of the gel used to represent the soft tissues. Several material candidates were considered for the bone structure. A nylon filament (PA6, Nylstrong by Smartfil, Spain) was ultimately selected for its mechanical and thermal properties (melting temperature in the range of 245°C to 265°C).

#### Manufacturing Phase – Bone Structure

The technique selected for 3D printing of the bones and the mold was Fused Filament Fabrication (FFF), an additive manufacturing process which uses thermoplastic and thermoset filaments to create 3D objects. The digital bone structure described previously was converted to a 3D-printable file in a .gcode format (LulzBot TAZ Pro, Aleph Objects, Loveland, CO) (Figure 4A). In order to allow for a smoother transition during manufacturing, additional geometric components were added to facilitate the articulation of the bones with

breakaway supports to maintain the bone orientation and reduce printer support clean up. After completion of the 3D printing process, the finger joints were coated with a silicon material to mimic ligaments, and the support material was removed to obtain the fully assembled bone structure (Figure 4C).

#### Manufacturing Phase – Two-Part Mold

The two-part mold was manufactured using the same FFF technique used for the bones. The two halves of the mold were printed separately. The synthetic gel melting temperature also drove the selection of the 3D printing material used for the mold. Several material candidates were considered, and ultimately polylactic acid (PLA) was selected. PLA has a melting temperature in the range of 130°C to 180°C, which ensured that the mold would not be distorted or damaged during gel casting. Two molds were manufactured: one for the specimens cast with gel # 0 and one for the specimens cast with gel #4 (Figure 5A-B).

#### Manufacturing Phase – Full Hand

After 3D printing the two-part mold, each of the halves was coated with a demolding agent to allow for easy removal of the finished product. Once the bone joints were cured, the bone hand was arranged in the mold, relying on the pins and pinholes to place and maintain the bone position within the hand cavity created by the two-part mold. A compressible silicon gasket was then placed between the mold halves before clamping them together,

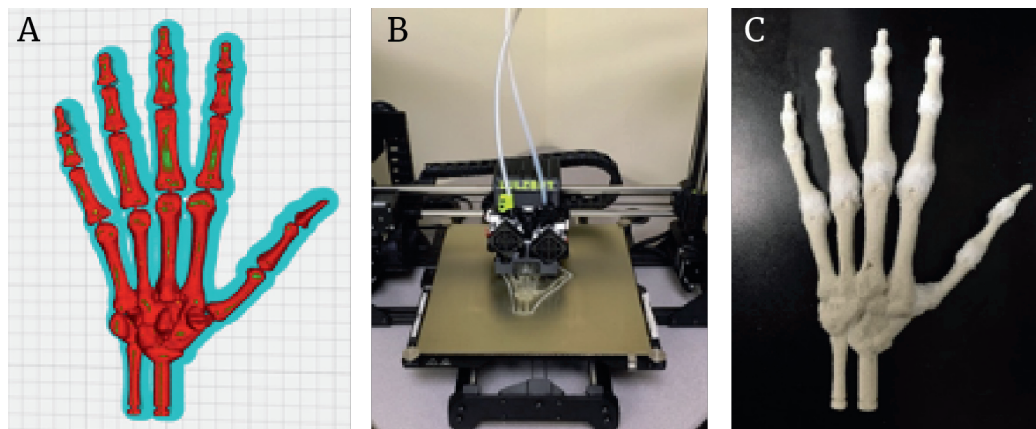


**Figure 4.** 3D printing of bone structure. (A) preparation in slicing software, (B) filament fusion fabrication, (C) finished 3D-printed bone structure

leaving the mold ready for the gel casting (Figure 5A). The synthetic gel was heated to 120°C until it liquified and then poured into the mold while the mold was tilted to allow smooth flow of material to each finger, as well as to facilitate the removal of air out of the hand cavity. After fully pouring the molten gel, percussive assistance was applied to complete the degassing of the gel as it cooled down. The resulting cast was left to cool down and cure for 24 hours before demolding. An identical procedure was applied for creating hands with gel #0 and gel #4 (Figure 5B-C).

## Results and Discussion

The procedure described in the previous section was implemented to initially manufacture five hand specimens using gel #0 and five specimens using gel #4. The specimens were weighed and measured to verify dimensional stability. For gel #0, the average weight was 462g (SD = 10g) and a coefficient of variation (COV = SD/average) of 2.3%. For gel #4, the average weight was 415g (SD = 8g), COV = 1.9%. The difference in weight between specimens with different gels is due to the difference in densities: 880.38 kg/m<sup>3</sup>, and 834.34 kg/m<sup>3</sup>, for gel #0 and gel #4, respectively. Moreover, the total lengths of the specimen and widths of the palm were also measured, and all specimens showed a COV of <1.0%. These results confirm that the molds did not distort during gel pouring and

maintained their original shape through multiple casts, thus maintaining dimensional stability.

The use of two types of medical-grade synthetic gel changed the overall stiffness of the resulting surrogate hand. A measure of the gel stiffness while in a solid state is known as the hardness of the gel. The Shore hardness scale is typically used for soft materials. In this scale, higher numbers on the scale indicate a higher resistance to indentation and thus a harder material. In contrast, lower numbers mean less indentation resistance and typically correspond to softer materials<sup>12</sup>. Gel #0 and gel #4 had reported average Shore ratings of 21.4 and 3.3, respectively. The hardness of each gel type controlled the overall flexibility of the hand. Notably, specimens manufactured with gel #4 displayed a flexibility closer to the flexibility of an actual hand.

The bone structure maintained its shape and position within the hand during the casting process, confirming the suitability of holding pins and pinholes to support the bones. One aspect observed in the specimens (using both gel types) was the bonding between the gel and bones: bonding at the fingers and fingertips appeared generally weaker than bonding at the knuckles and metacarpals. Importantly, this difference in bonding could affect overall hand model behavior during impact tests. In the future, addition of a bonding agent to the surface of the bones before pouring the gel may improve the

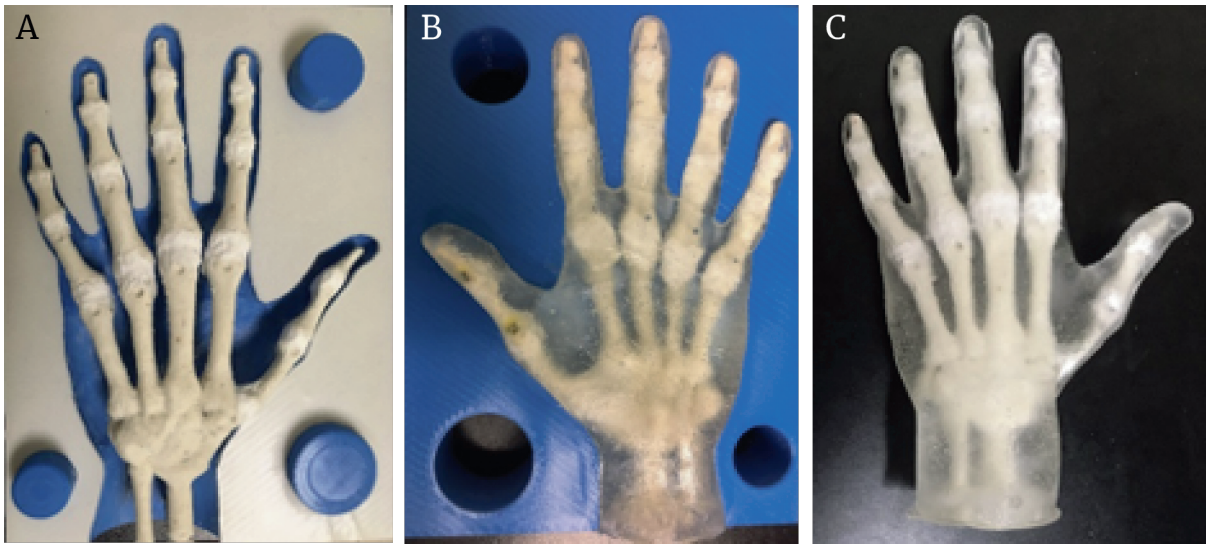


**Figure 5. Surrogate hand assembly.** (A) 3D printed bone assembly in place for gel casting, (B) palmar view of gel hand after demolding, (C) dorsal view of finished surrogate gel hand

adhesion between these materials.

Specimens were also subjected to controlled impacts to determine the range of impact reaction forces for unprotected hands following the procedure described previously<sup>6</sup>. Impacts were performed on interphalangeal (PIP) joints, metacarpophalangeal (MCP) joints, and at the midpoint of the metacarpal bones (MET). At each position for gel #0, the average impact reaction forces and standard deviation (SD) were 2856N (599N), 2193N (684N), and 1468N (634N), respectively. A set of preliminary impact tests were also performed on the specimens manufactured with gel #4. For these specimens, the average impact reaction forces and standard deviations were 2571N (104N), 1890N (125N), and 1325N (158N), respectively. Importantly, these values are in the range of 75% of the values reported in published literature for experiments performed with cadaveric hands (3835N for PIP joints and 2740N for MCP joints)<sup>14</sup>. In order to reduce this gap, further adjustments will be necessary for the 3D printing settings of the bone structure, to increase the strength of the surrogate bones and reduce the variability in the impact reaction forces seen in the specimens manufactured with gel #0.

## Conclusions

A methodology for creating a surrogate

hand which can be manufactured using 3D printing and gel casting techniques was presented. The physical models developed in this work can be quickly and readily reproduced using additive manufacturing for the bone structure and synthetic gel casts in a two-part mold for the soft tissue. The resulting surrogate hands were able to maintain dimensional stability after casting. With adjustments in the 3D printing settings of the bone structure, these surrogate hands can help further validate research on the impact-protective qualities of various metacarpal gloves. Furthermore, the techniques developed in this work can be refined to ensure consistent manufacturing, as well as expanded to other body parts to obtain valid and accurate substitutes for testing other protective systems. The digital models developed in this work also provide the basis for developing computational simulations and parametric studies for further evaluation of forces and damage resulting from an impact on the hand.

## Acknowledgments

This work was supported in part by the financial assistance from the Arch Coal Inc. Endowment for Mine Health and Safety Research in the Statler College of Engineering and Mineral Resources and administered by the Dept. of Mining and Industrial Extension.

## Competing Interests

The authors declare no competing interests.

## References

- Pollard, J., Heberger, J., et. al. (2014). Maintenance and repair injuries in US mining. *Journal of Quality in Maintenance Engineering*, 20(1), 20–31. <https://doi.org/10.1108/JQME-02-2013-0008>
- US Department of Labor (2018, March) Mine Safety and Health Administration – MSHA, Accident Injuries DataSet. <https://arlweb.msha.gov/OpenGovernmentData/OGIMSHA.asp>
- Sammarco, J. J., Podlesny, A., et. al. (2016). An analysis of roof bolter fatalities and injuries in US mining. *Trans. Soc. Min. Metall. Explor.*, 340(1), 11–20. <https://doi.org/10.19150/trans.7322>
- Dolez, P., Soulati, K., et. al. (2010). Studies and research projects, technical guide RG-738, information document for selecting gloves for protection against mechanical hazards. *Institut de recherché Robert-Sauvé en Santé et en Sécurité du Travail (IRSST)*, Montréal, Québec, Canada. <http://elcosh.org/record/document/3685/d001225.pdf>
- Loshek, P. D. (2015). Classification of adequate impact protection for hands. *Theses and Dissertations 974. University of Wisconsin Milwaukee*. <https://dc.uwm.edu/etd/974/>
- Sosa, E. M., Dean, J. M., et. al. (2019). Performance under impact loads of metacarpal gloves used in the mining industry. *Proceedings of the XXXIst Annual International Occupational Ergonomics and Safety Conference, New Orleans, Louisiana, USA, June 12-13, 2019*, 135-140. <http://isoes.info/2019/Papers/Sosa.pdf>
- Virtama, P., Kajanoja, P., et. al. (1960). Density of human carpal, metacarpal and digital bones. *Annales Medicinæ Experimentalis et Biologiae Fenniae*, 38, 467-471.
- Fox, K. M., Kimura, S., et. al. (1995). Radial and ulnar cortical thickness of the second metacarpal. *Journal of Bone and Mineral Research*, 10(12), 1930-1934. <https://doi.org/10.1002/jbmr.5650101212>
- Garret, J. W. (1971). The adult human hand: some anthropometric and biomechanical considerations. *Human Factors*, 13(2), 117-131. <https://doi.org/10.1177/001872087101300204>
- Gordon, C. C., Churchill, T., et. al. (1989). Anthropometric survey of US personnel: summary statistics, interim report, March 1989, 1-50. <https://apps.dtic.mil/dtic/tr/fulltext/u2/a209600.pdf>
- Greiner, T. M. (1991). Hand anthropometry of US army personnel. *Technical Report NATICK/TR-92/011*. <https://apps.dtic.mil/dtic/tr/fulltext/u2/a244533.pdf>
- Mix, A. W., & Giacomini, A. J. (2011). Standardized polymer durometry. *Journal of Testing and Evaluation*, 39(4), 696-705. <https://doi.org/10.1520/JTE103205>
- Bankoff, A. D. P. (2012). Biomechanical characteristics of the bone, in T. Goswami (Ed.), *Human Musculoskeletal Biomechanics* (Chapter 4, pp. 61-86). INTECH. <https://doi.org/10.5772/19690>
- Carpanen, D., Kedgley, A. E., et. al. (2016). The risk of injury of the metacarpophalangeal and interphalangeal joints of the hand, *Proceedings of the IRCOBI Conference 2016*. Paper IRC-16-110. <http://www.ircobi.org/wordpress/downloads/irc16/pdf-files/110.pdf>

---

## About the Author:

Trevor Brison is a Morgantown native studying mechanical engineering at the Statler College of Engineering and Mineral Resources. His fields of interest include biomedical science (specifically biomimicry and prosthesis), robotics, and material science. After graduating, Trevor intends to continue his education in specialized work environments or graduate school. In his free time, he explores other interests including food chemistry, specifically in fermentation, and chemicals which affect taste receptors.

---

## How to Cite This Article:

Brison, T. A., & Sosa, E. M. (2020). Development of surrogate hand for impact tests. *Mountaineer Undergraduate Research Review*, 5, 9-15.